

Trapping and Beamloading in hybrid Plasma Wakefield Accelerator schemes

Alexander Knetsch

October 21, 2016

CONTENTS

1.	<i>theory</i>	3
1.1	The history of wakefield acceleration	3
1.2	Plasma physics	3
1.2.1	debye shielding	3
1.2.2	time scales	3
1.2.3	plasma definition	3
1.2.4	electromagnetic waves in plasmas	3
1.2.5	fluid model of plasmas	3
1.2.6	waves in plasmas	3
1.2.7	wavebreaking	3
1.3	PWFA theory	4
1.3.1	history of PWFA	4
1.4	The blowout regime	4
1.5	Descriptions for the blowout regime	4
1.6	Accelerator physics	4
1.6.1	Panowsky-Wenzel Theorem	4
1.7	Electron Trapping in plasma accelerators	4
1.7.1	luminal wakefield, electron injected at rest	5
1.7.2	subluminal wakefield, electron injected at rest	6
1.7.3	subluminal wakefield, electrons at rest	6
1.7.4	superluminal wakefield	6
1.7.5	From the Trapping Potential to the Current Profile - velocity bunching at it's max.	6
1.8	laser ionisation description	6
1.8.1	Keldysh Parameter	6
1.8.2	ADK theory	7
1.9	Influence of the ionization behaviour	7
1.9.1	Rake injection	7
1.10	Trojan Horse	7
1.11	Downramp assisted Trojan Horse	7
2.	<i>experiment</i>	8
2.1	The FACET experimental setup	8
2.1.1	Laser energy calibration	8
2.2	Electro Optical Sampling (EOS)	10
2.3	Ionization test	12
2.4	Plasma glow diagnostic	12

1. THEORY

1.1 *The history of wakefield acceleration*

Tajima Dawson great Idee, MTV bubble regime, same time PWFA von Rosenzweig... first linear measurements for PWFA

1.2 *Plasma physics*

An introduction into plasma physics is given by starting with chens definition. Topics are

1.2.1 *debye shielding*

1.2.2 *time scales*

scattering can be talked about

1.2.3 *plasma definition*

There are different types of plasmas, but we are only handling with thin, cold weakly coupled plasmas

1.2.4 *electromagnetic waves in plasmas*

dispersion relation needs to be talked about. Especially the dispersion relation of lasers during ionization should get some insight here. One has to look into ionization defocussing.

1.2.5 *fluid model of plasmas*

1.2.6 *waves in plasmas*

So far everything still flows nicely with working along Chen and Mulser. However now the turn needs to be taken. The reason is wavebreaking

1.2.7 *wavebreaking*

Wavebreaking gives us the the ideal way to go from plasma description to blowout description.

1.3 PWFA theory

1.3.1 history of PWFA

A short historic overview is given. Maybe mention landau damping? Then of course, Tajima,Dawson. Also MTV and Rosenzweig should be mentioned.

1.4 The blowout regime

1.5 Descriptions for the blowout regime

Lotov, Suk, breakdown of fluid theory Q-tilde and resonant wake excitation.

1.6 Accelerator physics

Acc. physics should clearly be introduced. Emittance, brightness, twiss parameter need to be defined. Floettmann. A good book should be used here. Don't know which one,yet. TBD.

1.6.1 Panowsky-Wenzel Theorem

$$W_r = \partial_r W_z \quad (1.1)$$

This theorem is so important, it clearly needs a subsection. But where ?

1.7 Electron Trapping in plasma accelerators

In order to derive an expression for the trapping condition of a single electron in PWFA, one has to start with the equation of motion for such a single electron.

$$F = \frac{d\vec{p}}{dt} = q(\vec{E} \times \vec{B}) \quad (1.2)$$

with the electron charge q electric field \vec{E} and magnetic field \vec{B}

This leads to the single particle electron hamiltonian $H = \gamma mc^2 + \Phi$ with the temporal derivative.

$$\frac{dH}{dt} = \frac{d}{dt}(\gamma m_e c^2) + \frac{d}{dt}(q\Phi) \quad (1.3)$$

$$= \vec{v} \frac{d\vec{p}}{dt} + \frac{d}{dt}(q\Phi) \quad (1.4)$$

$$= q\vec{v}(-\nabla\Phi - \frac{\partial\vec{A}}{\partial t}) + \frac{\vec{v} \times \vec{B}}{c} + \frac{d}{dt}(q\Phi) \quad (1.5)$$

$$= q(\frac{d}{dt}\Phi - \vec{v}\vec{\nabla}\Phi - \vec{v}\frac{\partial\vec{A}}{\partial t}) \quad (1.6)$$

$$= q(\frac{\partial\Phi}{\partial t} - \vec{v}\frac{\partial\vec{A}}{\partial t}) \quad (1.7)$$

If one assumes now, that the wake fields are constant during the trapping process, then

$$\left(\frac{\partial}{\partial t} + v_\phi \frac{\partial}{\partial z}\right) f = f(z - v_\phi t) \quad (1.8)$$

$$\left(\frac{\partial}{\partial t} + v_\phi \frac{\partial}{\partial z}\right) f = 0 \quad \forall f(\vec{r}, z - v_\phi t) \quad (1.9)$$

which is especially true for the hamiltonian.

$$\begin{aligned} \frac{d}{dt} H &= q\left(\frac{\partial \Phi}{\partial t} - \vec{v} \frac{\partial \vec{A}}{\partial t}\right) \\ &= -qv_\phi\left(\frac{\partial \Phi}{\partial z} - \vec{v} \frac{\partial \vec{A}}{\partial z}\right) \end{aligned}$$

Since $H - v_\phi P_z = \text{const.}$

$$H - v_\phi P_z = \text{const.} \quad (1.10)$$

$$\gamma mc^2 + \Psi - v_\phi p_z - v_\phi q A_z = \text{const.} \quad (1.11)$$

$$\gamma + \frac{q\Phi}{mc^2} - v_\phi \frac{p_z}{mc^2} = \text{const.} \quad (1.12)$$

$$\underbrace{\gamma - v_\phi \frac{p_z}{mc^2} - \frac{q}{mc^2}(\Phi - v_\phi A_z)}_{\bar{\Psi}} = \text{const.} \quad (1.13)$$

$\bar{\Psi}$ is the trapping potential, that determines the potential difference for an electron in a potential that moves with a phase velocity v_ϕ with respect to the laboratory frame. It is valid for small as for relativistic velocities. With the trapping potential one can calculate if an electron inside the plasma wake will be accelerated or not i.e. if electrons will be able to catch up with the wake's velocity during the propagation of the wake or if it will slip out of the potential. From the prior calculations a general formula can be determined, that compares

$$\Delta \bar{\Psi} = \bar{\Psi}_i - \bar{\Psi}_f = \gamma_f - \gamma_i - \gamma_f \frac{v_\phi v_f}{c^2} + \gamma_i \frac{v_\phi v_i}{c^2} \quad (1.14)$$

In order to honor the name "trapping potential" i.e. to apply this derivation to make predictions of the electron trapping behavior in the plasma wake, it is necessary to define a trapping condition. An obvious and conventional choice is that an electron should catch up with the wake's velocity so that $v_f = v_\phi$. Equation 1.14 consequently simplifies to

$$\Delta \bar{\Psi} = \gamma_\phi - \gamma_i - \gamma_\phi \frac{v_\phi^2}{c^2} + \gamma_i \frac{v_\phi v_i}{c^2} \quad (1.15)$$

Equation 1.15 can be further separated into different physical cases:

1.7.1 luminal wakefield, electron injected at rest

In this case the plasma wake travels with a phase velocity near the speed of light, which is the case for beam-driven scenarios with high γ driver beams ($v_\phi \approx c$), and electrons starting inside the wake initially at rest ($v_i \approx 0$). Here Equation 1.15 simplifies to

$$\Delta \bar{\Psi} = -1 \quad (1.16)$$

Examples of this case are the underdense photocathode, or Trojan Horse injection [1], or wakefield induced ionization injection [2].

1.7.2 subluminal wakefield, electron injected at rest

$$\Delta\bar{\Psi} = \gamma_\phi \left(1 - \frac{v_\phi^2}{c^2}\right) - 1 = \gamma_\phi^{-1} - 1 \quad (1.17)$$

This formula can for example be applied to ionization injection in LWFA [3] or beam-driven ionization injection schemes in which the wake's phase velocity is retarded such as the Downramp-assisted Trojan Horse (DTH) [?], which this work has as special focus on. In latter case mathematically strictly speaking $\frac{dH}{dt} \neq 0$, but for small changes $\frac{dH}{dt} \approx 0$ during the injection process of the electrons, equation 1.17 can still be applied.

1.7.3 subluminal wakefield, electrons at rest

1.7.4 superluminal wakefield

There are physical situations imaginable in which the wake or at least part of the wake move with a phase velocity faster than the speed of light. This is the case for example when a beam driven wake traverses an electron density upramp. From the previous deductions it seems obvious, that trapping electrons in such a superluminal wakefield is not possible, as γ_ϕ^{-1} becomes complex for $v_\phi > c$.

However, if the superluminosity is only transient as with a short density upramp, the phase velocity will return to c right after the transition. In this case trapping can be possible, but the mathematic tool presented in this section is insufficient to describe the trapping and the phase velocity after the transition is setting the demand on the potential.

1.7.5 From the Trapping Potential to the Current Profile - velocity bunching at it's max.

emittance preservation

why don't you ... look at space charge effect to estimate required gamma/acceleration and focusing forces for emittance preservation ? Try looking at Pak's thesis and this emittance paper that claims one needs a fast acceleration, but knows nothing about Trojan Horse yet.

1.8 laser ionisation description

(see diss by Ihar Shchatsin in FU Berlin)

1.8.1 Keldysh Parameter

With E_{bind} being the binding energy and $U_p = \frac{q^2 I}{2m_e \epsilon_0 c \omega^2}$ being the ponderomotive energy

$$\gamma = \sqrt{\frac{E_{bind}}{2U_p}} \quad (1.18)$$

$\gamma > 1$ -> Multiphoton Ionisation
 $\gamma < 1$ tunnel ionisation or BSI

1.8.2 ADK theory

Tunnel ionization is great

1.9 Influence of the ionization behaviour

Here it is to be described how for TH the co-moving frame is advantagous. dependence of ionization front to create witness beams. Image of Ionization front.

1.9.1 Rake injection

It could be discussed here how a witness generation might be different for the wake electric fields. For example, there is no movement of the release position in x_i . But the release won't happen in the potential minimum.

1.10 Trojan Horse

1.11 Downramp assisted Trojan Horse

2. EXPERIMENT

In 2014 the experimental campaign for demonstrating the proof-of-concept of Trojan Horse injection (see 1.10) started at the Facility for Advanced Accelerator Experimental Tests (FACET) at the SLAC national laboratory as the experiment E210. It was a collaborative effort with researchers from the University of Hamburg, University of California Los Angeles (UCLA), University of Strathclyde Glasgow and Radiabeam technology with a devoted support from the SLAC personnel. The FACET experiments had to be designed to be non-excluding, which led to a fruitful joint learning process between several groups. It is fair to say that E210 was one of the most complex and accuracy-wise most demanding experiments conducted so far at FACET. Several steps were required in improving the overall setup, until the experiment was eventually successful. The most crucial obstacles to overcome were timing and alignment between two laser arms and the electron beam. The timing requirements between the electron beam and the pre-ionization laser are rather soft as long as the pre-ionization occurs before the arrival of the electron beam and with a timing difference less than the recombination time (ns-s range). However, proper control over relative time-of-arrival between the injection laser and the electron beam required - in principle - control over timing on the order of 10 fs. With an expected timing jitter in the range of 200 fs the best solution here was to accurately measure the relative TOA with an electro-optical sampling (described in 2.2) to determine the injection properties from the data, rather than hope for live-control. For finding the synchronization (t_0) as well as fine-alignment between electron beam and injection laser, a newly observed effect on the plasma glow described in 2.4 was measured and applied.

2.1 *The FACET experimental setup*

2.1.1 *Laser energy calibration*

The FACET laser system ... The energy that can be used on target of the OAP is controlled at two points in the laser-beamline. At each point a cube-polarizer is surrounded by two $\lambda/2$ -waveplates, where the upstream one is motorized. The main energy waveplate is located in the laser-room and the probe-energy waveplate is located in the tunnel area shortly after the split between main laser path and probe laser path at the main sampler, which means that the probe laser energy is determined by both waveplate settings while the main laser energy is set by the main laser energy waveplate only. From the power-meter in the laser-room, that measures shot-by-shot laser pulse energy, all the way down to the tunnel a variety of optical components are used until the laser is finally focused onto the target. The typical shot-to-shot laser energy jitter is $\approx 5\%$ FWHM.

Manta Cameras: [4]

All measured losses in optical components combined with the fitted functions for the waveplate energies (see figure 2.1) combined give the on target energy applicable by axilens and OAP

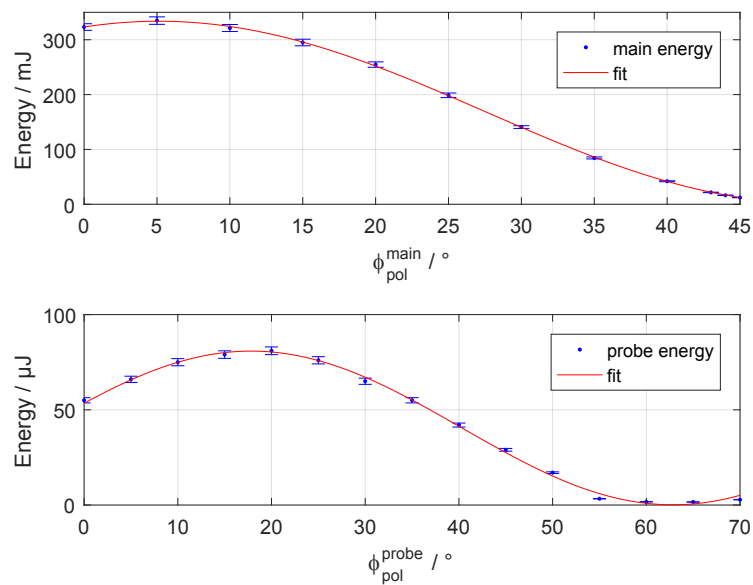


Fig. 2.1: Laser energy calibration for main energy waveplate (upper plot) and probe energy waveplate (lower plot)

respectively.

$$\begin{aligned} W_{\text{Laser}}^{\text{OAP}} &= W_{\text{Laser}}^{\text{Laserroom}} \times 1.25 \times 10^{-2} \\ &\times \left(0.994 \cos^2 \left(\frac{2\pi}{180} (\phi_{\text{pol}}^{\text{main}} + 66.9) \right) + 1.16 \times 10^{-3} \right) \\ &\times \left(0.998 \cos^2 \left(\frac{2\pi}{180} (\phi_{\text{pol}}^{\text{probe}} - 17.8) \right) + 1.62 \times 10^{-3} \right) \end{aligned}$$

$$W_{\text{Laser}}^{\text{Axilens}} = W_{\text{Laser}}^{\text{Laserroom}} \times 0.253 \quad (2.1)$$

$$\times \left(0.994 \cos^2 \left(\frac{2\pi}{180} (\phi_{\text{pol}}^{\text{main}} + 66.9) \right) + 1.16 \times 10^{-3} \right) \quad (2.2)$$

$$(2.3)$$

This means that for a typical laser energy output of 500 mJ a maximum energy of 6.2 mJ on OAP target and 125.9 mJ on axilens could be used.

2.2 Electro Optical Sampling (EOS)

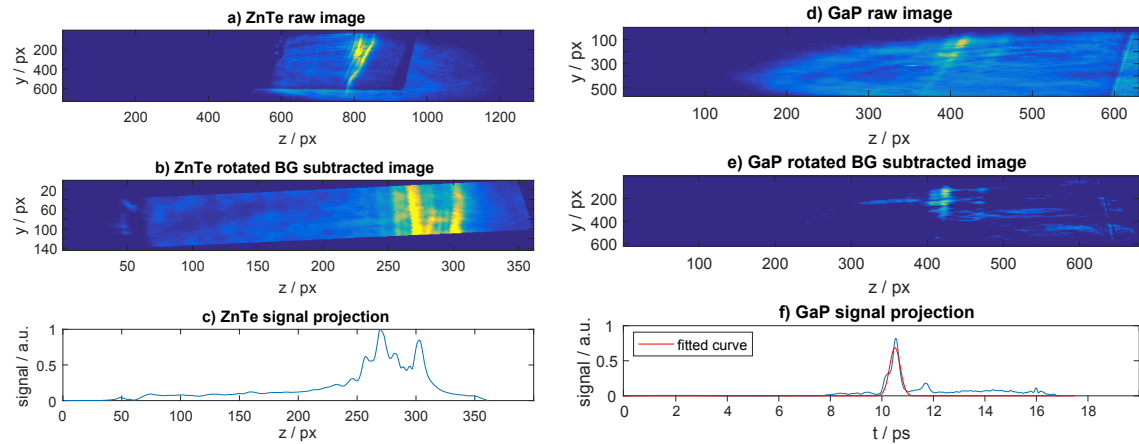
In order to measure the relative time-of-arrival between electron bunch and laser pulse, a non-destructive shot-to-shot diagnostic was necessary. Electro-optical sampling is an excellent choice for sub-picosecond electron bunches [5]. An externally applied electric field to crystals like GaP and ZnTe induces a birefringence in the optical axis of the material. This effect is called the pockels, or electro-optic effect. In this experiment the crystal is located in close proximity (few mm distance) to the electron beam axis. Due to the high $\gamma_b \approx 42000$, the beam electric field is strongly lorentz-contracted and can be assumed to temporally only extend for the length of the electron beam. Consequently the electric field applied to the crystal and with that the induced birefringence are only active while the electron beam passes by the crystal. A linear polarized laser pulse, traversing the crystal at the same time will change its polarization and is analyzed by a polarizing filter.

The crystal plate is oriented perpendicular to the electron beam axis to minimize temporal overlap and the laser has an $\approx 40^\circ$ angle with the electron beam which enables a correlation between signal position i.e. the part of the laser with rotated polarization and relative timing.

The entire ladder supports a YAG crystal to find the electron beam axis, a 500 m thick ZnTe for broad timing scans and GaP with 100 m thickness for fine resolution. A detailed description of the physics involved in the application of electro-optical crystals as TOA and bunch length diagnostic can be found in [6].



Fig. 2.2: Setup of upstream electro-optical sampling inside the picnic basket chamber. Electron beam (green) and EOS laser (red) co-propagate in a small angle



2.3 Ionization test

2.4 Plasma glow diagnostic

One huge advantage of the hydrogen FACET setup compared to the oven setup is that now several view ports allow for observing the interaction or ??.

The plasma glow diagnostic as a very simple tool, that turned out to be extremely helpful in controlling the alignment and synchronization of the experimental setup. The main idea is to have a camera integrate over the recombination light. It was observed that this

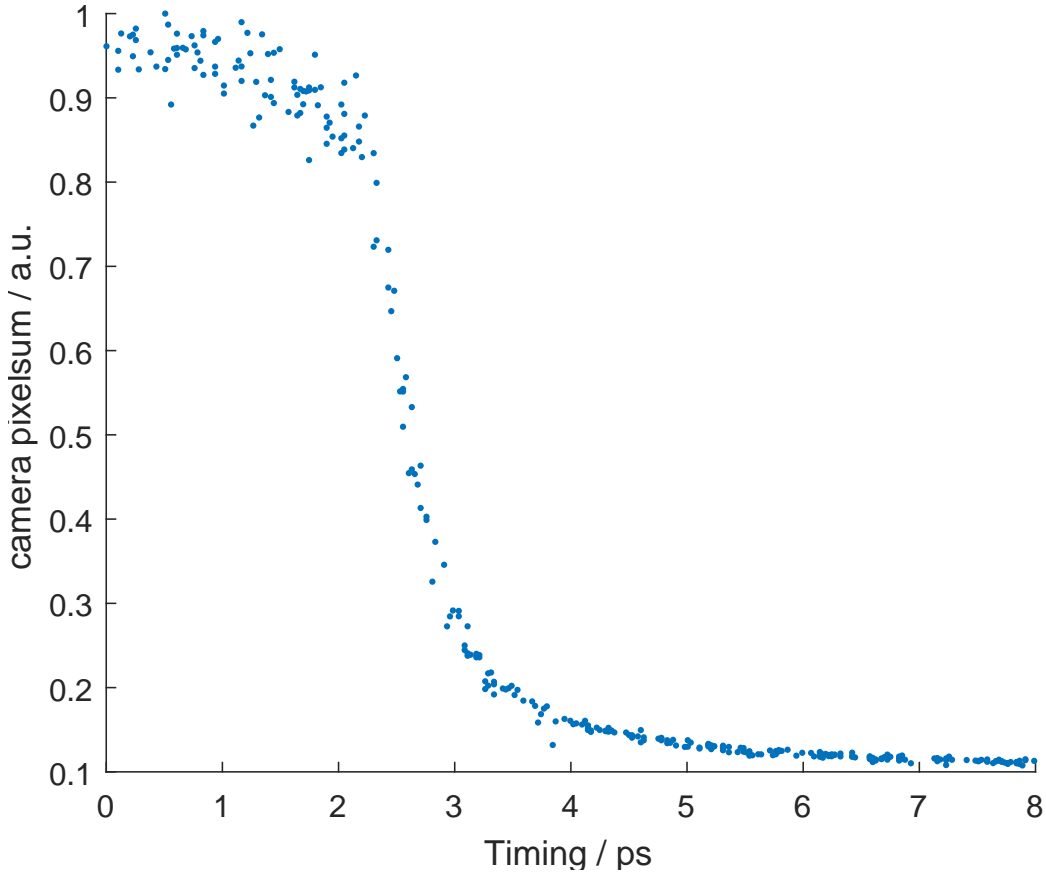


Fig. 2.3: Relative electron beam to injection laser timing scan. The pixel counts measured by the cube 3 vertical camera with a 656 ± 10 nm band-pass filter are sorted by the EOS. evaluation.

Figure 2.3 shows the plasma glow accumulated intensity at the wavelength 656 ± 10 nm , sorted by relative time-of-arrival between electron beam as measured by the EOS. The transition between a situation where the injection laser arrives earlier than the electron beam and vice versa is around 1 ps wide, which sufficiently fulfills the requirements to find a range of synchronization as the total

range of the EOS crystal is around 20 ps ????. During the data acquisition the electron beam charge was 3.1 ± 0.17 nC.

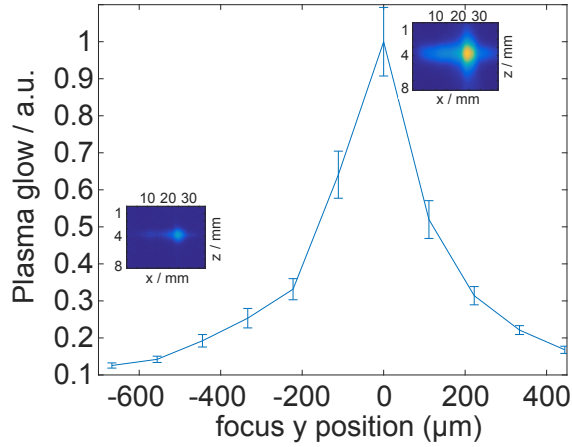


Fig. 2.4: Plasma glow in 4 torr H₂ measured by vertical camera in cube 3. The injection laser off-axis parabola roll is scanned. The vertical plasma position is evaluated by the focus diagnostic.

Result:

With the [7]

BIBLIOGRAPHY

- [1] B. Hidding, G. Pretzler, J. B. Rosenzweig, T. Königstein, D. Schiller, and D. L. Bruhwiler. Ultracold electron bunch generation via plasma photocathode emission and acceleration in a beam-driven plasma blowout. *Phys. Rev. Lett.*, 108:035001, Jan 2012.
- [2] A. Martinez de la Ossa, C. Behrens, J. Grebenyuk, T. Mehrling, L. Schaper, and J. Osterhoff. High-quality electron beams from field-induced ionization injection in the strong blow-out regime of beam-driven plasma accelerators. *Nuclear Instruments and Methods in Physics Research Section A: Accelerators, Spectrometers, Detectors and Associated Equipment*, 740:231 – 235, 2014. Proceedings of the first European Advanced Accelerator Concepts Workshop 2013.
- [3] A. Pak, K. A. Marsh, S. F. Martins, W. Lu, W. B. Mori, and C. Joshi. Injection and trapping of tunnel-ionized electrons into laser-produced wakes. *Phys. Rev. Lett.*, 104:025003, Jan 2010.
- [4] Allied Vision, <https://www.alliedvision.com/en/products/cameras/detail/Manta/G-125.html>. *Manta G-125 Data sheet*.
- [5] X. Yan, A. M. MacLeod, W. A. Gillespie, G. M. H. Knippels, D. Oepts, A. F. G. van der Meer, and W. Seidel. Subpicosecond electro-optic measurement of relativistic electron pulses. *Phys. Rev. Lett.*, 85:3404–3407, Oct 2000.
- [6] Bernd Richard Steffen. *Electro-Optic Methods for Longitudinal Bunch Diagnostics at FLASH*. PhD thesis, University of Hamburg, 2007.
- [7] Eric Esarey and Mark Pilhoff. Trapping and acceleration in nonlinear plasma waves. *Physics of Plasmas (1994-present)*, 2(5):1432–1436, 1995.